Pressuremeter and Shallow Foundations on Stiff Clay

JEAN-LOUIS BRIAUD, KENNETH E. TAND, AND ERIK G. FUNEGARD

The bearing capacity and settlement rules for the design of shallow foundations on stiff clays using the results of pressuremeter tests are reviewed. The results of 17 footing tests on 8 stiff clays are used, together with pressuremeter test results to evaluate the existing rules. New simplified bearing capacity rules are proposed. Menard's equation for settlement is proven reasonably accurate. An elasticity approach to settlement calculations using the pressuremeter modulus is proposed.

The pressuremeter can be used for the design of shallow foundations on stiff clays. Rules of design were developed in the early 1960s by Menard and his coworkers. These rules were adjusted in the mid-1970s by the Laboratoire des Ponts et Chaussées. In this paper the rules of design using pressuremeter test results for shallow foundations on stiff clays are examined in light of recent footing tests. Both bearing capacity and settlement considerations are addressed; adjusted bearing capacity rules are proposed, as well as an alternative settlement approach.

PRESSUREMETER TEST AND PARAMETERS

Several different types of pressuremeters exist. The preboring pressuremeter, the selfboring pressuremeter, and more recently the sampler and cone pressuremeters. This paper deals only with the preboring pressuremeter whereby the probe is inserted in an open borehole. Once inserted, the probe is inflated and pushes radially against the borehole wall. The plot of the radial stress at the cavity wall versus the relative increase in probe radius is the typical result of a pressuremeter test (PMT) after proper account of membrane stiffness and volume corrections. Standard procedures for preparing the borehole, performing the test, and reducing the data have been proposed *(1–3)*. It is recommended that any pressuremeter curve be plotted as shown in Figure 1 because this type of curve allows any pressuremeter data to be compared and the pressuremeter parameters to be calculated without any additional information on the probe dimensions.

From the pressuremeter curve, two main parameters are calculated: the pressuremeter modulus E_o and the net limit pressure p_L^*. The modulus E_o is obtained from the straight part of the curve (AB in Figure 1) using the equation based on the expansion of a cylindrical cavity in an isotropic homogeneous elastic space:

$$E_o = (1 + \nu)\,(p_2 - p_1)\,\{[1 + (\Delta R/R_o)_1]^2 + [1 + (\Delta R/R_o)_2]^2\}/[1 + (\Delta R/R_0)_1]^2 - [1 + (\Delta R/R_o)_2]^2 \qquad (1)$$

where

ν = Poisson's ratio, usually taken equal to 0.33;
R_o = deflated radius of the probe;
p_1, $(\Delta R/R_o)_1$ = coordinates of the point at the beginning of the straight line on the curve (A in Figure 1); and
p_2, $(\Delta R/R_o)_2$ = coordinates of the point at the end of the straight line on the curve (B in Figure 1).

The limit pressure p_L is defined as the pressure reached when the initial volume of the cavity has been doubled. This corresponds to a value of $\Delta R/R_o$ equal to $0.41 + 1.41\,(\Delta R/R_o)_1$. The net limit pressure p_L^* is

$$p_L^* = p_L - p_{OH} \qquad (2)$$

where p_{OH} is the total horizontal pressure at rest (Figure 1).

In addition, a reload modulus E_R is often obtained from the slope of the unload reload loop (CD in Figure 1). The value of E_R is calculated by using Equation 1 applied to points C and D instead of A and B in Figure 1.

It must be emphasized that the preparation of a quality pressuremeter borehole is the single most important step in the use of the pressuremeter in design. The error in foundation behavior predictions induced by the design rules themselves is much less than the error that can be induced by using the results of poor quality pressuremeter tests; this is especially true for settlement predictions because the modulus E_o is more sensitive to borehole disturbance than the limit pressure. Therefore it is essential that pressuremeter tests be performed only by experienced personnel. A suggested practice for the preparation of a pressuremeter borehole has been proposed *(1)*.

CORRELATIONS BETWEEN PRESSUREMETER, STANDARD PENETRATION, AND CONE PENETROMETER TESTS

A data base of pressuremeter test data and other test data was formed. The pressuremeter data were collected over the last 10

J. L. Briaud, Civil Engineering Department, Texas A&M University, College Station, Tex. 77843. K. E. Tand, Kenneth E. Tand and Associates, Inc., 1408 E. North Belt Drive, Suite 150, Houston, Tex. 77032. E. G. Funegard, Amoco Research Center, Amoco Corporation, P.O. Box 400, Naperville, Ill. 60566.

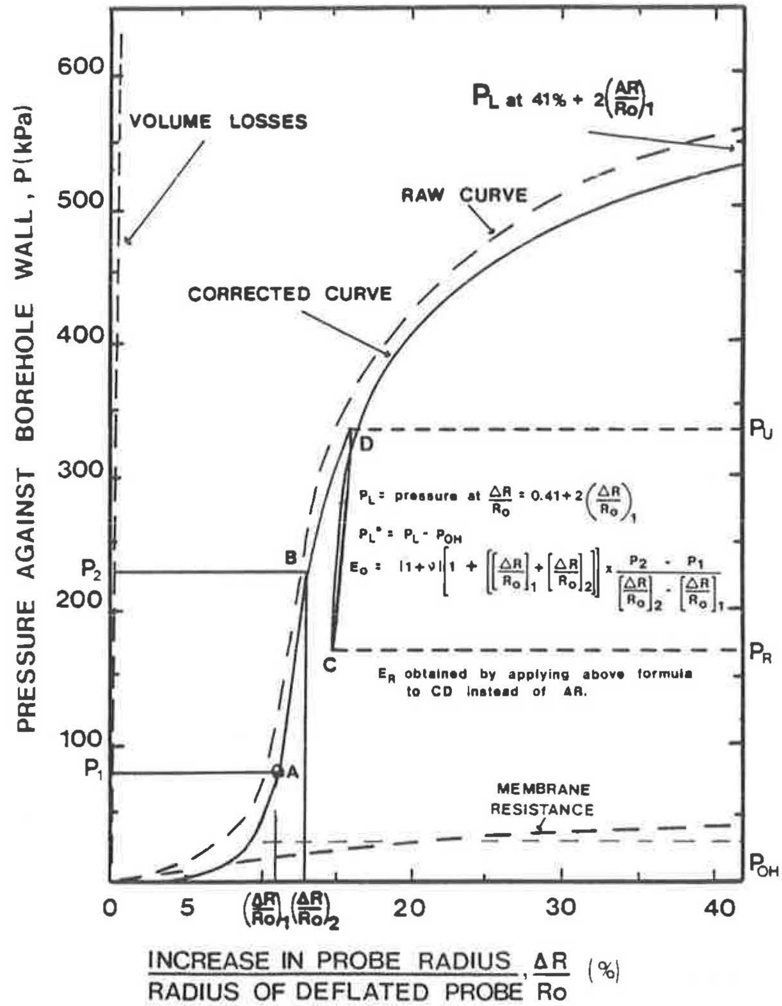

FIGURE 1 Typical preboring pressuremeter test curve.

years on various research and consulting projects. The pressuremeters used were the Menard, the TEXAM, and the pavement pressuremeters. The 82 pressuremeter borings were located in the south, southwest, west, and central United States with 36 sand, 44 clay, and 2 silt sites. Other borings were performed next to the PMT borings, leading to data on undrained shear strength s_u, effective stress friction angle ϕ, standard penetration test (SPT) blow count N, and cone point and friction resistance qc and fs. A record was created at each depth in a boring, which consisted of E_o, E_R, p_L, s_u, Φ, qc, and fs. A total of 463 records were accumulated. The data are described in detail by Briaud et al. *(4)*. Best fit linear regressions were performed for combinations of any two parameters. Of interest are the following equations for clays:

$$p_L = 7.5\ S_U \tag{3}$$

$$E_o = 100\ S_U \tag{4}$$

$$E_R = 300\ S_U \tag{5}$$

$$p_L = 0.2\ qc \tag{6}$$

$$E_o = 2.5\ qc \tag{7}$$

$$E_R = 13\ qc \tag{8}$$

The scatter involved in the preceding correlations is large as shown by the example in Figure 2. These correlations must not be used in design; they are presented only to give an idea of the order of magnitude of the pressuremeter parameters compared with other soil parameters.

BEARING CAPACITY: ORIGINAL RULES

The approach proposed by Menard *(5)* is to relate the ultimate capacity of a footing, q_L, to the net limit pressure obtained from the pressuremeter

$$q_L = k\ p^*_{Le} + q_o \tag{9}$$

where p^*_{Le} is the equivalent net limit pressure within the zone of influence of the footing, k is the bearing capacity factor, and q_o is the total stress overburden pressure at the footing depth. The value of p^*_{Le} is to be obtained by

$$p^*_{Le} = (p^*_{L1} \times p^*_{L2})^{1/2} \tag{10}$$

where p_{L1} is the average net limit pressure within ± 0.5B above

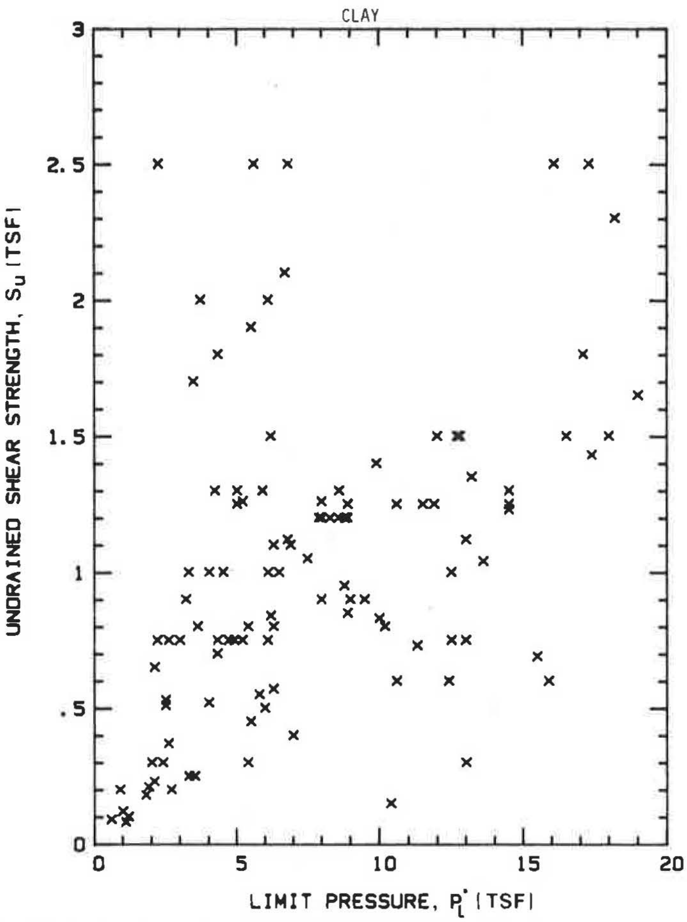

FIGURE 2 Example of correlations from the data base.

and below the footing depth and p_{L2} is the average net limit pressure within 0.5B to 1.5B below the footing level where B is the footing width. Menard *(5)* originally proposed a chart giving k as a function of relative embedment H_e (Figure 3), where H_e is the effective embedment depth calculated as

$$H_e = 1/p^*_{Le} \sum_{o}^{D} p^*_{Li}\,\Delta z_i \tag{11}$$

where D is the embedment depth of the footing, and p^*_{Li} is the net limit pressure in a Δz_i thick layer within the depth of embedment. This definition of H_e allows layers within the depth of embedment to be taken into consideration; these layers are stronger or weaker than the layer on which the footing is resting.

BEARING CAPACITY: PRESSUREMETER VERSUS UNDRAINED STRENGTH APPROACH

The preceding approach is to be compared with the undrained shear strength-plasticity theory approach:

$$q_L = N_c S_U + \gamma D \tag{12}$$

The term $N_c S_U$ in Equation 12 compares directly with the term k_p^*Le in Equation 9. For surface circular footing, the factor N_c is 6.2 *(6)*, the factor k is 0.8 (Figure 3). This leads to a value of p^*_{Le} equal to 7.75 S_U, which compares very favorably with the 7.5 S_U of Equation 3 for the data base.

The factor N_c increases as the depth of embedment of the footing increases. N_c reaches a maximum of 9 at a depth of embedment to width of footing ratio D/B of 4 *(6)*. The k value

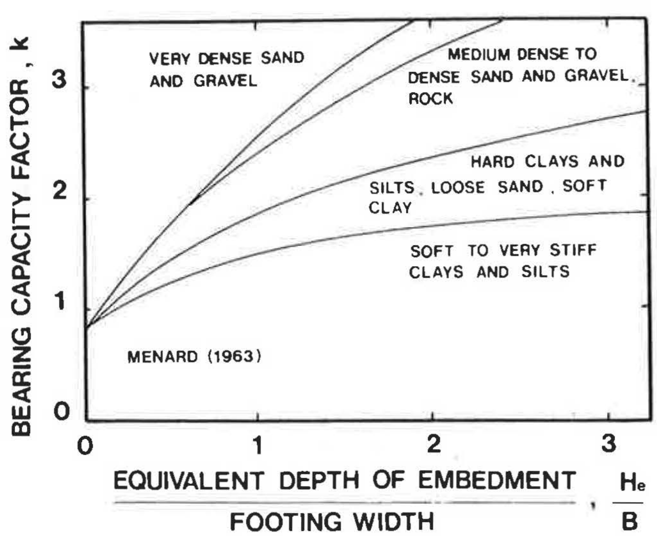

FIGURE 3 Bearing capacity factor *(5)*.

would then be expected to reach a maximum value of 9/6 × 0.8 = 1.16 at D/B of 4. Figure 3 shows a k value much larger than 1.16 for a D/B of 4.

Another factor influencing the ultimate bearing pressure, q_L, is the compressibility of the clay; an N_c factor that depends on a compressibility index, I, was proposed by Vesic *(7)*. This was done in an effort to correct for the shortcomings of the rigid-plastic solution. This important factor is incorporated directly into p_{Le} because the compressibility of the clay affects the pressuremeter limit pressure. Indeed the theoretical expression of p_L in the case of undrained behavior is

$$p_L = p_o + S_U\ [1 + \mathrm{Ln}(G/S_U)] \tag{13}$$

BEARING CAPACITY: RECENT LOAD TEST RESULTS

In 1978 Baguelin et al. *(8)* updated Menard's rules (Figure 4). Since then footing tests have become available that were not included in Menard's 1963 rules nor the Laboratoire des Ponts et Chaussées (LPC) 1978 rules (Table 1).

Shields and Bauer *(9)* reported the results of two footing tests on a stiff sensitive clay. The first footing was a 0.46-m (1.5 ft) diameter rigid plate (Figure 5). The test was performed at the bottom of a 1.3-m (4.26 ft) wide, 2.6-m (8.52 ft) deep trench. The second footing was a 3.1 × 3.1-m (10.2 ft × 10.2 ft) square, 0.66-m (2.2 ft) thick concrete footing at the ground surface (Figure 6). The soil was an overconsolidated sensitive clay with the following average properties: undrained shear strength from vane tests 110 kPa (1.12 tsf), water content 43 percent, and unit weight 18 kN/m^3 (114.6 pcf). The pressuremeter test results are shown in Figures 5 and 6 together with the test configuration and the load settlement curves.

O'Neill and Sheikh *(10)* reported the results of a drilled shaft test on a stiff clay. The 0.762-m (2.5 ft) diameter shaft was 2.36 m (7.75 ft) deep with a 2.41-m (7.92 ft) diameter bell (Figure 7). The soil was a stiff clay with the following average properties: undrained shear strength from unconsolidated undrained triaxial tests 86 kPa (0.88 tsf), water content 22 percent, unit

TABLE 1 SHALLOW FOOTINGS DATA BASE

Study No.	Footing I.D. No.	Reference	Soil	Footing Width (m)	Footing Depth (m)	Footing Type
1	1	Deschenes	Medium	0.30	0	Strip
	2	Briaud	Dense	0.30	0.30	Strip
	3	*(24, 25)*	Sand	0.30	0.60	Strip
	4			0.30	0.90	Strip
2	5	Deschenes	Dense	0.30	0	Strip
	6	Briaud	Sand	0.30	0.30	Strip
	7	*(24, 25)*		0.30	0.60	Strip
3	8	Amar-Baguelin	Silt	1.0	0	Square
	9	Canepa *(18)*		1.0	0.60	Square
	10			1.0	1.0	Square
4	11	Shields-Bauer	Clay	0.46	2.6	Circular
	12	*(9)*		3.1	0.70	Square
5	13	O'Neill-Sheikh, Briaud *(10, 11)*	Clay	2.41	2.36	Circular
6	14	O'Neill-Reese,	Clay	0.76	7.0	Circular
	15	WCC *(12, 13)*		2.29	7.0	Circular
7	16	Tand-Funnegard	Clay	0.60	1.50	Circular
	17	Briaud *(14, 15)*		0.60	1.50	Circular
	18			0.60	1.50	Circular
8	19	Menard *(5)*	Sand/ Silt	0.25- 0.6	0.5- 1.7	Circular
9	20	Marsland-Randolph	Clay	0.865	6.1	Circular
	21	*(16)*		0.865	12.2	Circular
	22			0.865	18.3	Circular
	23			0.865	24.0	Circular
10	24	Johnson *(17)*	Clay	0.762	0.0	Circular

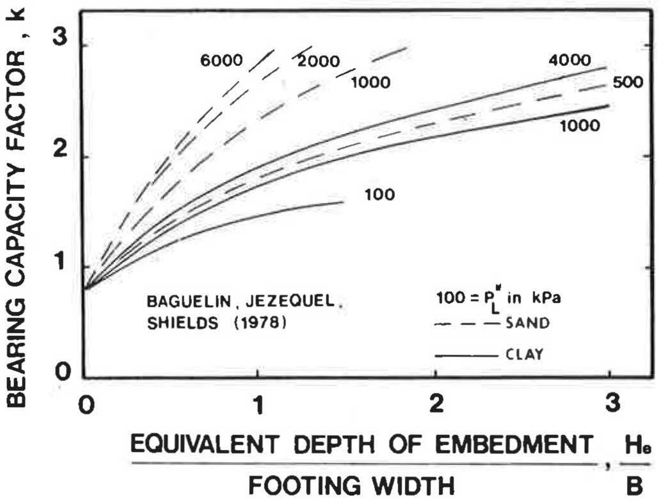

FIGURE 4 Bearing capacity factor *(8)*.

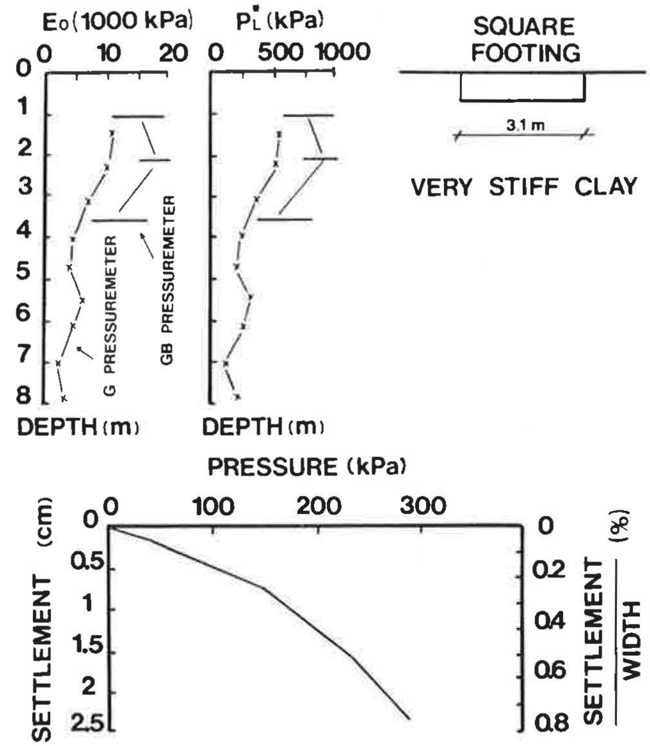

FIGURE 6 Shields-Bauer footing test *(9)*.

weight 19.8 kN/m^3 (126 pcf), and cone point resistance 2700 kPa (27.6 tsf). The test configuration and the load settlement curves obtained at the base of the bell are shown in Figure 7. Briaud and Riner *(11)* reported the results of pressuremeter tests at the same site; these results are shown in Figure 7.

O'Neill and Reese *(12)* reported the results of two drilled shaft tests on a stiff clay. The first drilled shaft was 7 m (23 ft) deep and 0.762 m (2.5 ft) in diameter (Figure 8). The second shaft was identical to the first shaft except for a 2.29-m (7.5 ft) diameter bell (Figure 9). The soil was a stiff clay with the following average properties within the zone of interest: undrained shear strength from unconfined compression tests 98 kPa (1 tsf), water content 24 percent, and unit weight 20.4 kN/m^3 (130 pcf). The test configuration and the load settlement curves obtained at the base of the shafts are shown in Figures 8 and 9. Woodward Clyde Consultants *(13)* performed a series of pressuremeter and cone penetrometer tests at the same site. The average cone point resistance close to the point of the shaft was

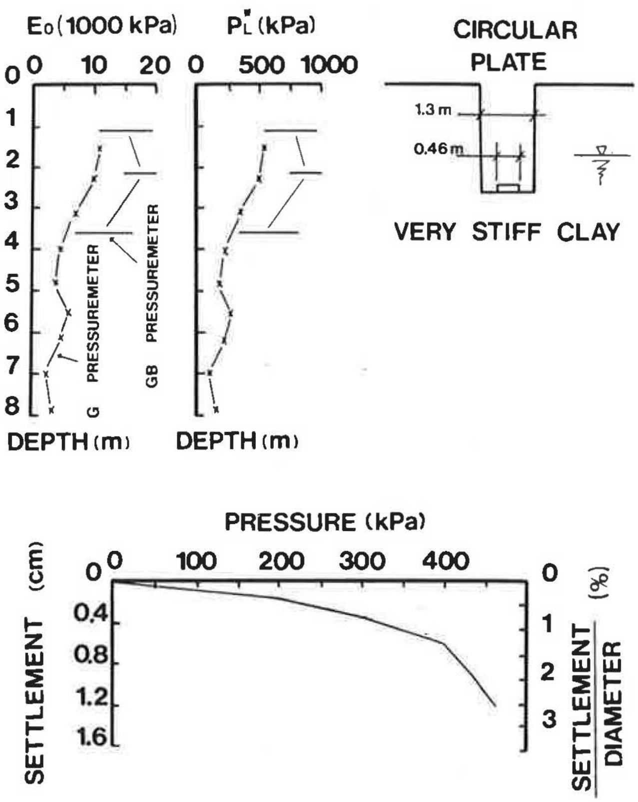

FIGURE 5 Shields-Bauer plate test *(9)*.

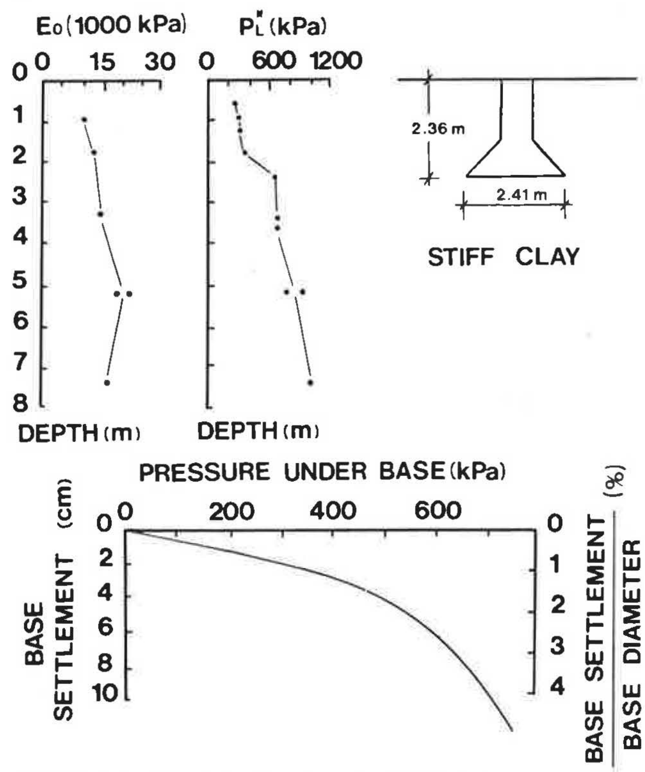

FIGURE 7 O'Neill-Sheikh-Briaud test *(10, 11)*.

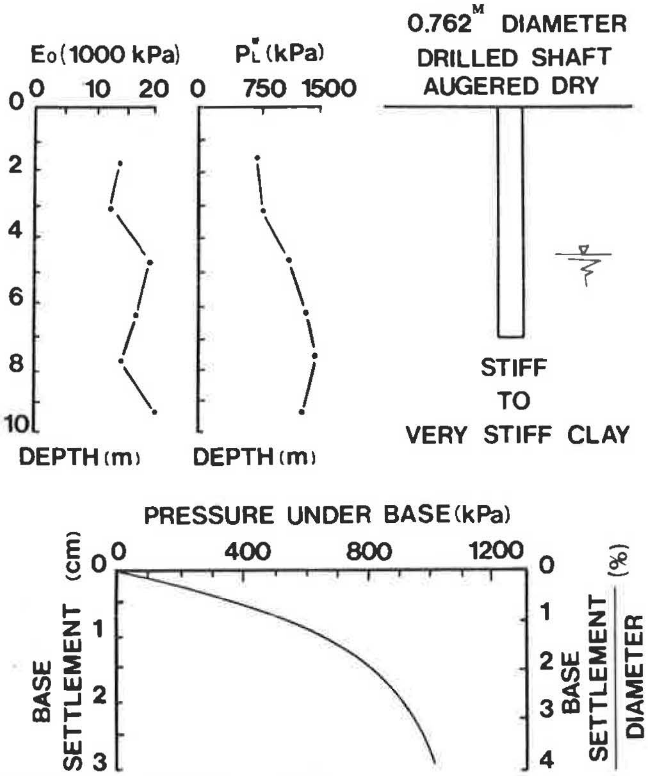

FIGURE 8 O'Neill-Reese-WCC test on straight drilled shaft *(12, 13)*.

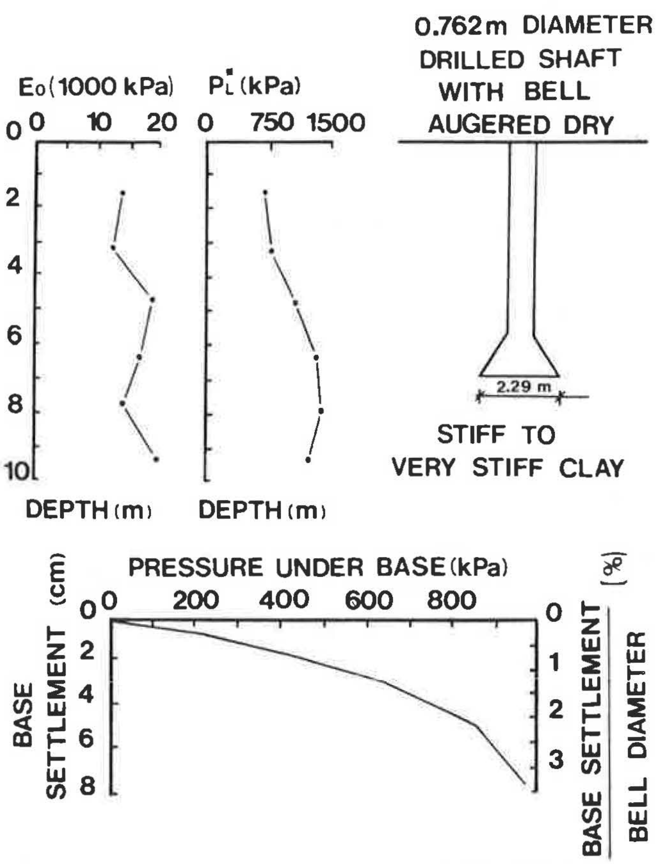

FIGURE 9 O'Neill-Reese-WCC test on belled drilled shaft *(12, 13)*.

3900 kPa (40 tsf); the pressuremeter test results are shown in Figures 8 and 9.

Tand et al. *(14)* reported the results of plate load tests at three sites (A, B, and C). The plate was 0.6 m (2 ft) in diameter and was placed at the bottom of a 0.6-m (2 ft) diameter, 1.5-m (5 ft) deep-cased hole (Figures 10, 11, and 12). At Site A, the soil was a stiff sandy clay with the following average properties: undrained shear strength from unconsolidated undrained triaxial tests 58.3 kPa (0.59 tsf), water content 20 percent and unit weight 19.5 kN/m^3 (124 pcf). At Site B, the soil was a medium sandy clay: undrained shear strength from unconsolidated undrained triaxial tests 38 kPa (0.39 tsf), water content 19.5 percent and unit weight 19.6 kN/m^3 (125 pcf). At Site C, the soil was a stiff clay: undrained shear strength from unconsolidated undrained triaxial tests 61.5 kPa (0.63 tsf), water content 25 percent, and unit weight 19.8 kN/m^3 (126 pcf). The test configuration and the load-settlement curves obtained are shown in Figures 10, 11, and 12. Briaud Engineers *(15)* reported the results of pressuremeter tests performed at Sites A, B, and C. These pressuremeter test results are shown in Figures 10, 11, and 12.

Marsland and Randolph *(16)* reported the results of plate load tests at four different depths in one uncased borehole (Table 1). The plate was 0.865 m (2.85 ft) in diameter. The soil was a very stiff fissured clay (London clay) with a unit weight of 19.6 kN/m^3 (125 pcf) and an undrained shear strength derived from the plate tests averaging 100 kPa (1 tsf). The pressuremeter test results are shown in Figure 13. Plate tests were performed at depths of 6.1, 12.2, 18.3, and 24 m (20, 40, 60, and 78.7 ft). The load settlement curve for the 18.3-m (60

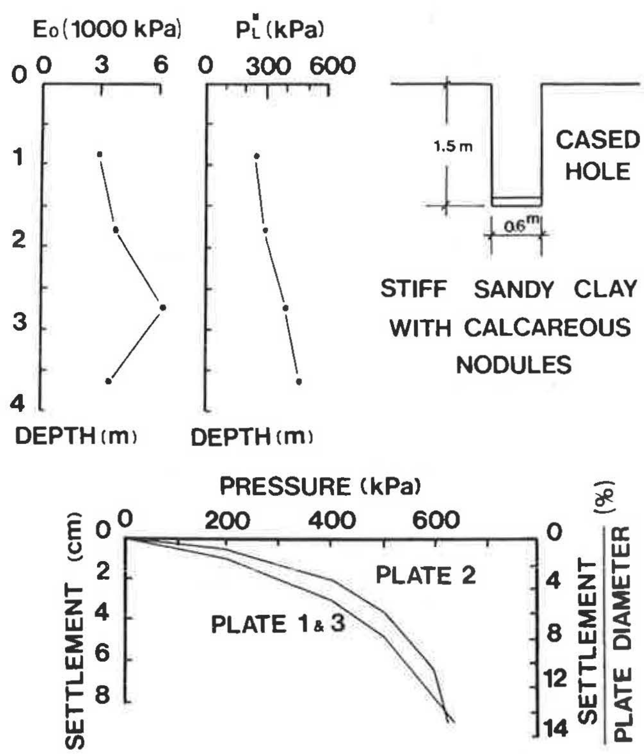

FIGURE 10 Tand-Funegard-Briaud plate tests (Texas City, Site A) *(14, 15)*.

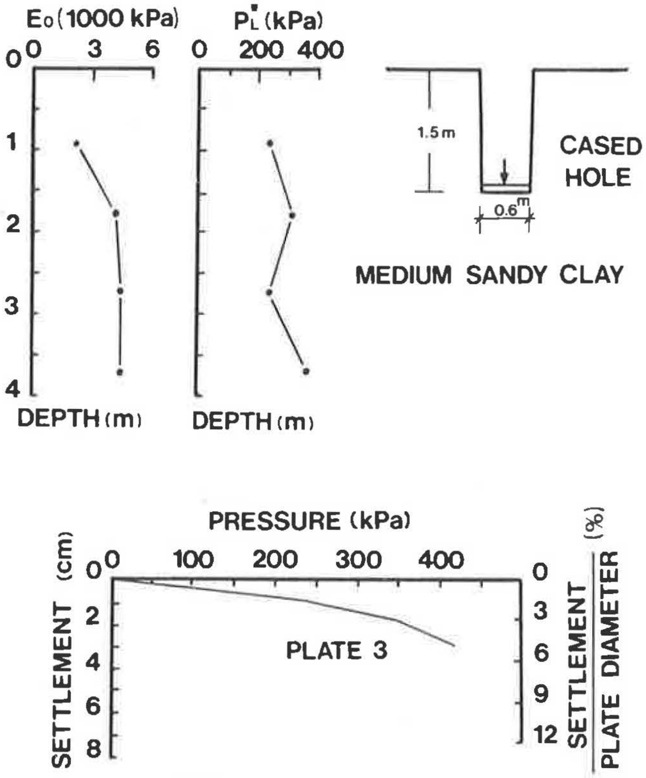

FIGURE 11 **Tand-Funegard-Briaud tests (Texas City, Site B)** *(14, 15).*

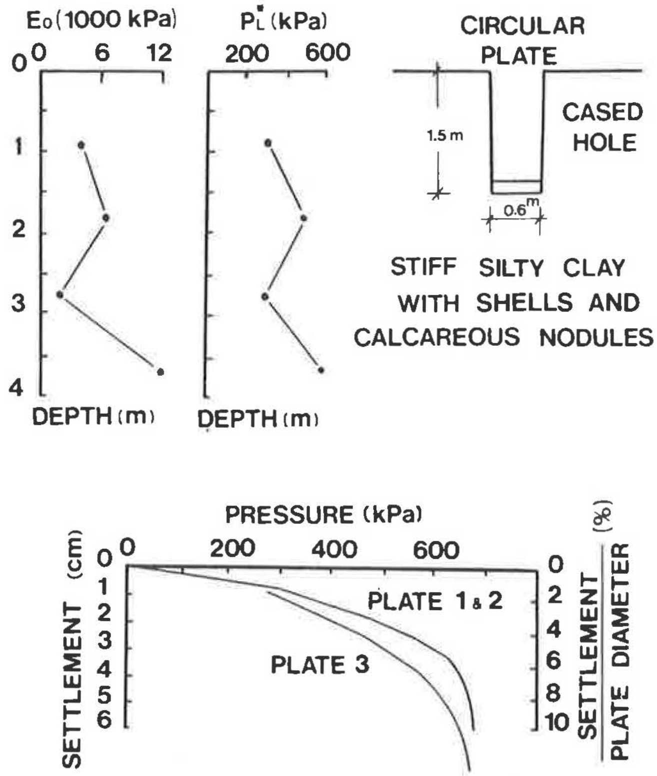

FIGURE 12 **Tand-Funegard-Briaud tests (Chocolate Bayou, Site C)** *(14, 15).*

ft) deep plate test was reported only by Marsland and Randolph (Figure 13) *(16)*. Johnson *(17)* reported the results of a plate load test on a stiff clay. The plate was 0.762 m (30 in.) in diameter and was placed at the surface of the clay (Figure 14). The soil was a stiff clay with the following average properties: undrained shear strength from undrained triaxial tests 100 kPa (1 tsf), water content 28 percent, plasticity index 45 percent, and dry unit weight 15 kN/m^3 (96 pcf). The pressuremeter test results are shown in Figure 14. The plate was not brought to failure.

BEARING CAPACITY: PROPOSED DESIGN CURVES

The ultimate bearing pressure, q_L, is defined here as the pressure reached for a settlement equal to one-tenth of the footing width (B/10). This is consistent with failure criterions used for pile load test analysis. Sometimes, especially in sands, the pressure increases past this value of q_L; however, settlements larger than B/10 are rarely obtained in footing tests, and this definition provides a consistent way of defining the ultimate bearing pressure. For each of the footing test results described previously, q_L as defined earlier, was determined. The equivalent limit pressure p^*_{Le} was calculated according to Equation 10, the effective embedment depth H_e was calculated according to Equation 11, and the overburden pressure q_o at the footing depth was also calculated. The values of q_L, p^*_{Le}, H_e, and q_o are given in Table 2 with additional results for silt and sand.

Using Equation 9, it was then possible to backfigure the

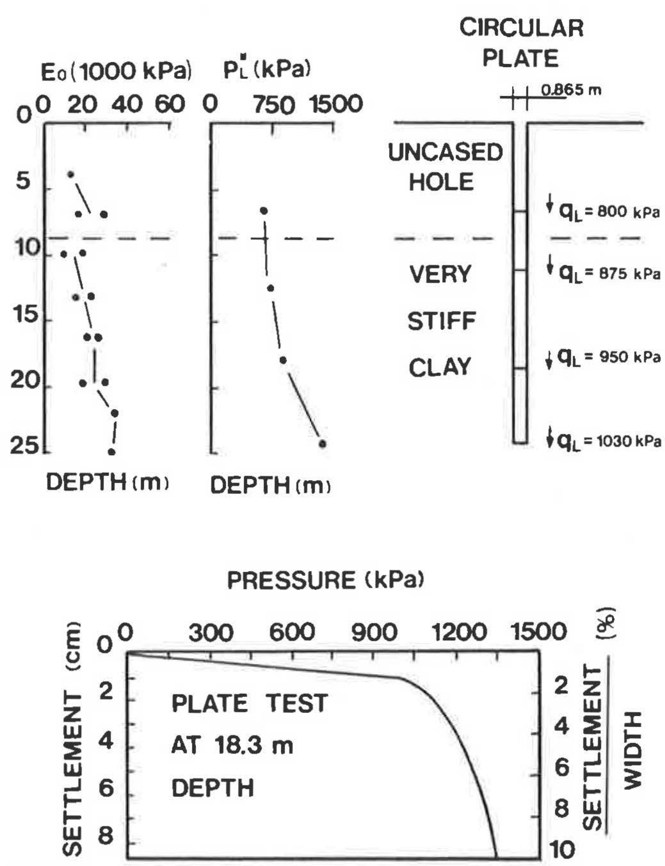

FIGURE 13 **Marsland-Randolph plate tests** *(16).*

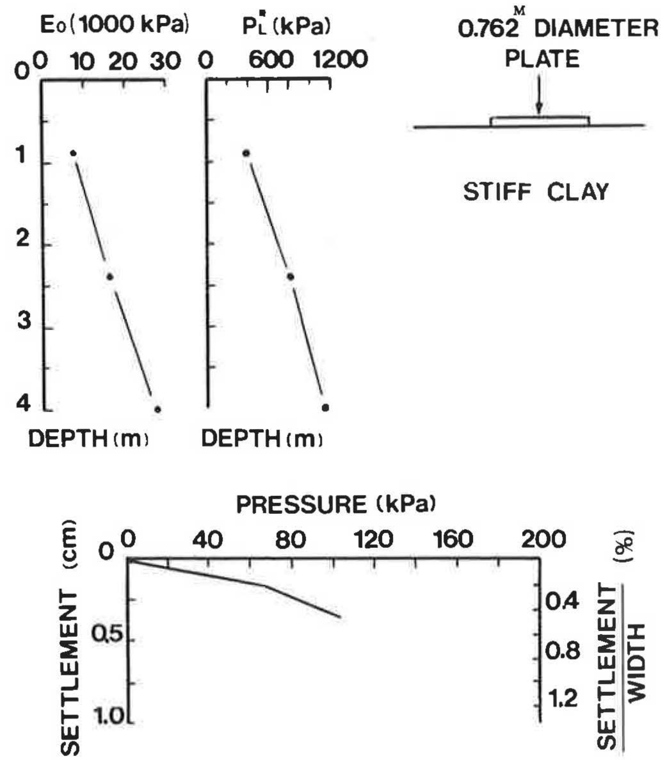

FIGURE 14 Johnson-Briaud plate test *(17)*.

measured bearing capacity factor k for each footing test (Table 2). The data points were then plotted as shown in Figure 15. After consideration of all the data available, the design curves shown in Figure 15 were selected. These curves correspond approximately to the curve that would split the data points in half (mean) minus one standard deviation of the scatter around the mean. It is emphasized that these curves are proposed to calculate the ultimate bearing pressure as defined by the one tenth of the width settlement criterion. It is also emphasized that the rules for obtaining p^*_{Le} and H_e must be followed rigorously.

By comparing Figures 3, 4, and 15, it can be seen that the proposed design curves are somewhat more conservative than the previous rules. The ratio of the ultimate bearing pressure predicted by these design curves to the measured ultimate bearing pressure varied between the extreme values of 0.60 to 1.24 for this data base. For comparison purposes, the precision of the method that consists of using the general bearing capacity equation to predict the ultimate bearing pressure is shown in Figure 16 for clay and in Figure 17 for sand. These figures come from a data base study conducted by Amar et al. *(18)*. As can be seen, the ratio of predicted overmeasured ultimate bearing pressure varies from 0.51 to 1.67 in clay and from 0.12 to 12 in sand. Therefore the pressuremeter may not improve significantly the bearing capacity predictions in clay but may improve dramatically the predictions in sand.

TABLE 2 SUMMARY OF ULTIMATE CAPACITY DATA FOR FOOTING LOAD TESTS

Study (1)		Soil (2)	Equivalent Net Limit Pressure p^*_{Le} (kPa) (3)	Bearing Pressure at B/10 Penetration q_L (kPa) (4)	Overburden Pressure q_o (kPa) (5)	Effective Embedment H_e/B (6)	Measured Bearing Capacity Factor k (7)
1 Deschenes-Briaud	F1C	Sand	152(43)	130	0.0	0.0	0.86
(24, 25)	F2C	Sand	167(60)	165	4.5	0.94	0.96
	F3C	Sand	174(107)	430	9.0	1.81	2.42
	F4C	Sand	192(149)	430	13.5	2.61	2.17
2 Deschenes-Briaud	F1D	Sand	407(86)	450	0.0	0.0	1.1
(24, 25)	F2D	Sand	424(126)	510	4.8	0.87	1.19
	F3D	Sand	447(252)	640	9.6	1.90	1.41
3 Amar-Baguelin-Canepa	F1	Silt	369	335	0.0	0.0	0.91
(18)	F2	Silt	389	375	13.0	0.56	0.93
	F3	Silt	393	450	21.0	0.92	1.09
4 Shields-Bauer *(9)*	(.45)	Clay	600	550	0.0	0.0	0.86
	(3.1)	Clay	561	550	12.3	0.28	0.96
5 O'Neill-Sheikh-Briaud *(10, 11)*		Clay	515	820	46.2	0.61	1.50
6 O'Neill-Reese-WCC	(0.762)	Clay	1256	1250	137.2	6.76	0.89
(12, 13)	(0.29)	Clay	1130	1225	137.2	2.43	0.96
7 Tand-Funegard-Briaud	A	Clay	286	560	30.0	2.18	1.85
(14, 15)	B	Clay	266	525	30.0	2.21	1.86
	C	Clay	376	660	30.0	1.99	1.68
8 Menard *(5)*		Sand	-	-	-	-	-
9 Marsland-Randolph	6.1	Clay	640	920	120	6.6	1.25
(16)	12.2	Clay	725	1095	240	12.2	1.18
	18.3	Clay	885	1310	360	15.6	1.08
	24.0	Clay	1360	1510	480	16.3	0.75
10 Johnson *(17)*	PB4	Clay	475 1	-	0.0	0.0	-

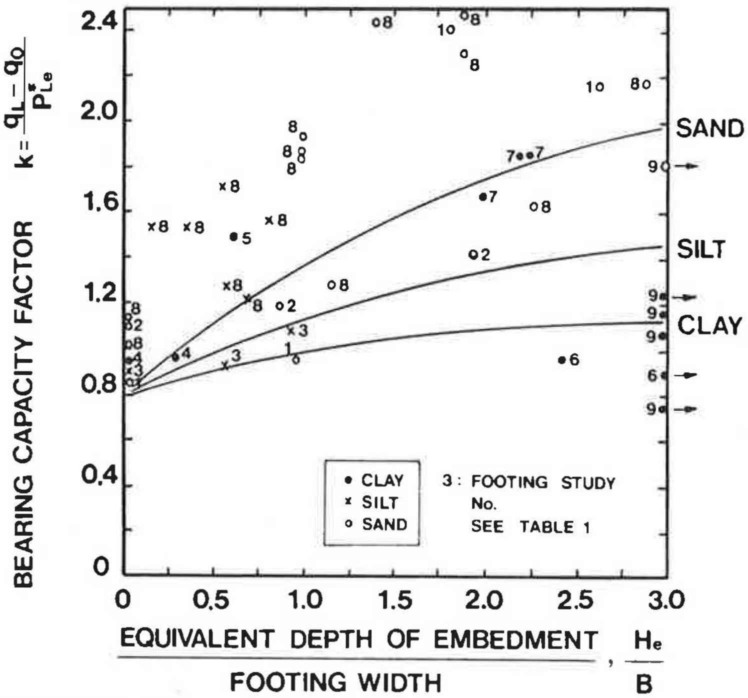

FIGURE 15 Recommended design curves for bearing capacity.

SETTLEMENT: MENARD'S APPROACH

In 1962, Menard and Rousseau *(19)* proposed a method of calculating the settlement of a footing on the basis of pressuremeter test results. The basis of Menard's settlement equation is related to the following theoretical background *(19, 8)*.

Two settlements can be considered: an undrained or no-volume change settlement, s_u, which takes place rapidly, and a drained or final settlement, s_T. In elasticity, s_u would be calculated by using undrained parameters (E_u, ν_u, G_u) and s_T by using drained-long-term parameters (E', ν', G), where E is Young's modulus, ν is Poisson's ratio, and G is the shear modulus.

The stress tensor (σ) at any point within the loaded mass of soil can be decomposed into its spherical (σ_s) and deviatoric component (σ_d):

$$\sigma = \sigma_s + \sigma_d \tag{14}$$

In elasticity the stress-strain relations can be written

$$\sigma_s = 3K\varepsilon_s = E/3\ (1 - 2\nu)\ \varepsilon_S \tag{15}$$

$$\sigma_d = 2G\varepsilon_d = E/1 + \nu\ \varepsilon_d \tag{16}$$

where K is bulk modulus, ε_s is spherical strain tensor, and ε_d is deviatoric strain tensor.

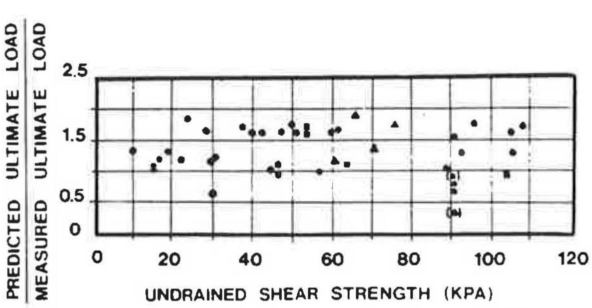

FIGURE 16 Measured versus predicted capacity by $q_u = N_c\ s_u + \gamma D$ for clay *(18)*.

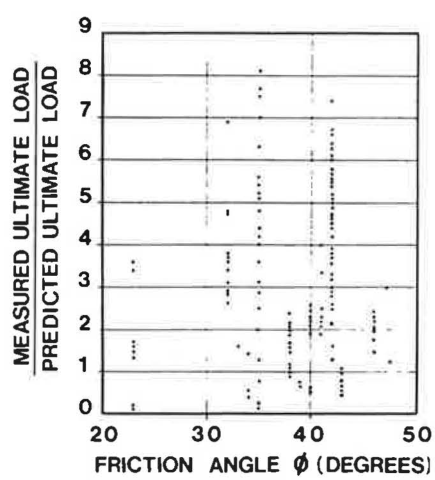

FIGURE 17 Measured versus predicted capacity by $q = 0.5\ \gamma BN_\gamma + \gamma DN_q$ for sand *(18)*.

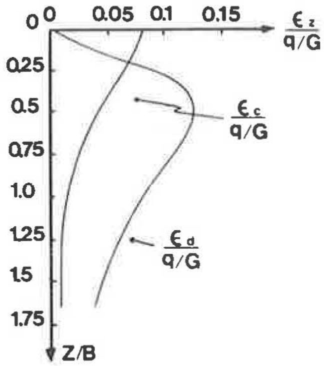

FIGURE 18 Deviatoric and spherical strains versus depth *(8)*.

Variation of the components ε_s and ε_d of the vertical strains ε_z are shown in Figure 18. The deviatoric component of the stress tensor, σ_d, is the same whether it is expressed in effective stress or total stress. Therefore

$$\sigma_{du} = \sigma_d' = \sigma_d \tag{17}$$

Since

$$\sigma_{du} = 2G_u\varepsilon_d \tag{18}$$

and

$$\sigma_d' = 2G'\varepsilon_d \tag{19}$$

then

$$G_U = G' = G \tag{20}$$

Consider the settlement of a rigid circular plate on an elastic half space

$$s_T = (\pi/8)/(1 - \nu'/G)\ qB \tag{21}$$

$$s_u = (\pi/8)/(1 - 0.5/G)\ qB \tag{22}$$

The difference $s_T - s_u$ is the consolidation settlement s_c

$$s_u = (\pi/16)\ (qB/G) \tag{23}$$

$$s_c = \pi/16\ (1 - 2\nu')\ qB/G \tag{24}$$

$$s_T = (\pi/16)\ (qB/G) + \pi/16\ (1 - 2\nu')\ qB/G \tag{25}$$

For an average Poisson's ratio (ν') of 0.33, s_u is three times larger than s_c and therefore represents 75 percent of the total settlement, s_T; this shows that when the width of the foundation is small compared to the depth of the compressible layer (most common case for shallow footings), the undrained settlement is the major portion of the final settlement.

The foregoing discussion of the settlement problem is the backbone of the pressuremeter equation for settlement *(19)*:

$$s = \underbrace{2qB_o(\lambda_d\ B/B_o)^{\alpha}/9E_d}_{\text{deviatoric settlement}} + \underbrace{\alpha q\lambda_c\ B/9E_c}_{\text{spherical settlement}} \tag{26}$$

where

- s = footing settlement,
- E_d = pressuremeter modulus within the zone of influence of the deviatoric tensor,

TABLE 3 MENARD'S α FACTOR *(8, 20)*

Soil Type	Peat		Clay		Silt		Sand		Sand and Gravel	
	E/p^*_L	α	E/p^*_L	α	E/p^*_L	α	E/p^*_L	α	E/p^*_L	α
Over-consolidated			>16	1	>14	2/3	>12	1/3	>10	1/3
Normally consolidated	For all Values	1	9-16	2/3	8-14	1/2	7-12	1/3	6-10	1/4
Weathered and/or remoulded			7-9	1/2		1/2		1/3		1/4

Rock	Extremely Fractured	Other	Slightly Fractured or Extremely Weathered
	α = 1/3	α = 1/2	α = 2/3

q = footing net bearing pressure q_{net},
B_o = reference width of 2 ft or 60 cm,
B = footing width,
α = rheological factor (Table 3),
λ_d = shape factor for deviatoric term (Figure 19),
λ_c = shape factor for spherical term (Figure 19), and
E_c = pressuremeter modulus within the zone of influence of the spherical tensor.

This equation is the elasticity Equation 25, which has been altered to take into account the footing scale effect $B\alpha$ and the magnitude of the pressuremeter modulus.

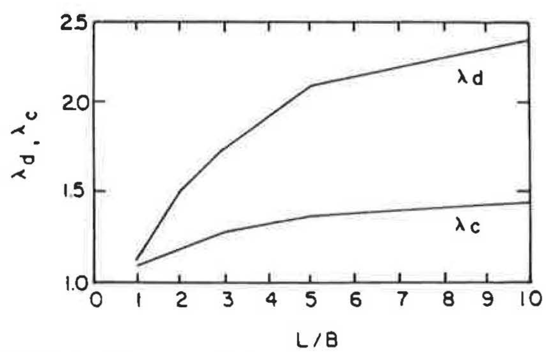

FIGURE 19 Shape factors *(19)*.

SETTLEMENT: PRESSUREMETER VERSUS CONSOLIDATION TEST APPROACH

Consolidation settlement is the result of the spherical part of the stress tensor. As can be seen from Figure 18, the spherical strain ε_c decreases rapidly with depth, indicating that consolidation settlement is prevalent at shallow depth only (e.g., one-half footing width, B/2, below the footing). On the other hand, the deviatoric strain, ε_d, remains significant down to at least 2B below the footing (Figure 18).

The consolidation test applies well to the prediction of ε_c, while the pressuremeter test, which is theoretically a pure deviatoric test, applies well to the prediction of ε_d. Therefore, for a wide foundation over a thin compressible layer where ε_c will predominate, the consolidation test approach is to be favored. For footings on deep relatively uniform deposits where ε_d will predominate, the pressuremeter test approach is to be favored.

Further acknowledging this distinction, Menard recommends that in Equation 26, E_d be taken as the average pressuremeter modulus over a significant depth below the footing, while E_c is the average modulus just below the footing. The averaging technique for E_d is based essentially on the ε_d distribution. The modulus E_c is empirically corrected into E_c/α in order to obtain a "consolidation" modulus. The details of the step-by-step procedure for calculating E_d and E_c can be found in discussions by Menard *(20)*, Briaud et al. *(2)*, and Baguelin et al. *(8)*.

SETTLEMENT: MENARD'S PREDICTION VERSUS LOAD TEST RESULTS

In 1978, Baguelin et al. *(8)* presented the results of 45 comparisons between predicted and measured settlements on various structures; the results are plotted in Figure 20.

The footing load tests presented earlier for bearing capacity evaluation were used to calculate the settlement by Menard's Equation 26. The procedure followed was to use the proposed design curves of Figure 15 in order to obtain a bearing capacity factor k, calculate the ultimate bearing capacity, and use a factor of safety of 3 to obtain the safe bearing pressure q_{safe} (Column 3, Table 4)

$$q_{safe} = k\, p^*_{Le}/3 + q_o \tag{27}$$

The pressure q_{safe} was then used to calculate the footing settlement (Column 4, Table 4). This settlement was compared with the settlement measured at q_{safe} during the load tests (Column 6, Table 4). Figure 21 is a comparison of measured and predicted settlement for the load tests described in this

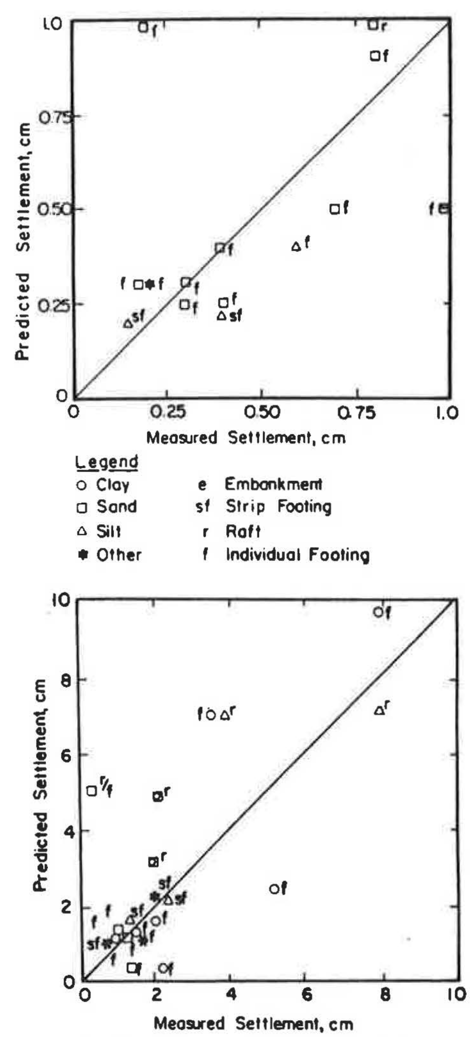

FIGURE 20 Measured versus predicted settlement by Menard's method *(8)*.

TABLE 4 SUMMARY OF SETTLEMENT DATA FOR FOOTING TESTS

Study (1)		Soil (2)	Calculated Safe Bearing Pressure q_{safe} (kPa) (3)	Calculated Settlement (Menard) S_{CM} (cm) (4)	Calculated Settlement (Elasticity) S_{CE} (cm) (5)	Measured Settlement at q_{safe} (cm) (6)	Factor of Safety (chosen) (7)	Factor of Safety (true) (8)
1 Deschenes-Briaud *(24, 25)*	F1C	Sand	40	0.58	1.45	0.5	3	3.25
	F2C	Sand	81	0.75	1.7	1.2	3	2.10
	F3C	Sand	108	0.8	1.48	0.4	3	4.25
	F4C	Sand	137	0.9	1.4	0.9	3	3.37
2 Deschenes-Briaud *(24, 25)*	F1D	Sand	108	0.75	1.69	0.6	3	4.17
	F2D	Sand	192	1.14	2	1.2	3	2.70
	F3D	Sand	266	1.28	2.16	1.3	3	2.46
3 Amar-Baguelin-Canepa *(18)*	F1	Silt	98	0.47	1.25	0.8	3	3.41
	F2	Silt	145	0.64	1.41	0.8	3	2.74
	F3	Silt	168	0.69	1.34	0.65	3	2.92
4 Shields-Bauer *(9)*	(0.46m)	Clay	160	0.24	0.33	0.14	3	3.44
	(3.1m)	Clay	171	1.9	2.25	1.0	3	3.39
5 O'Neill-Sheikh-Briaud *(10, 11)*		Clay	204	1.04	1.28	1.2	3	4.90
6 O'Neill-Reese-WCC *(12, 13)*	(0.762m)	Clay	639	0.77	1.08	0.95	3	2.22
	(2.29m)	Clay	557	1.6	2.43	2.5	3	2.59
7 Tand-Funegard-Briaud *(14, 15)*	A	Clay	133	0.55	0.66	0.5	3	5.14
	B	Clay	126	0.56	0.66	0.48	3	5.15
	C	Clay	165	0.56	0.61	0.48	3	4.67
8 Menard *(5)*		Sand	-	-	-	-	-	-
9 Marsland-Randolph *(16)*	18.3	Clay	702	0.81	0.70	0.79	3	2.78
10 Johnson *(17)*	PB4	Clay	126	0.35	0.50	0.50	3	-

paper, as well as additional tests in sand and silt. Figure 21 shows that a precision of ± 50 percent can be expected from Menard's rules.

Column 8 in Table 4 indicates the true factors of safety that were obtained by using the proposed bearing capacity design curves of Figure 15 and a chosen factor of safety of 3.

SETTLEMENT: ELASTICITY APPROACH

An alternative to Menard's settlement approach would be to use the elasticity formula *(21)*:

$$S = I_o I_1 (1 - \nu^2)\, q\, (B/E_o) \tag{28}$$

where

- S = the footing settlement,
- I_o and I_1 = influence factors,
- ν = Poisson's ratio,
- q = the bearing pressure,
- B = footing width, and
- E = pressuremeter modulus within the zone of influence.

Equation 28 was used to calculate the settlement of the footings under q_{safe} (Column 5, Table 4). The factors I_o and I_1 were obtained from Jambu et al. *(21)* using a length-to-diameter ratio of 20 for strip footings and a depth of hard-layer-to-diameter ratio of 20 for infinitely deep deposits (Figure 22). The average pressuremeter modulus, E_o, was obtained by following the averaging technique proposed by Schmertmann *(22)* together with his recommended strain distribution.

The resulting settlements are listed in Column 5 of Table 4. Figure 23 is a plot of predicted versus measured settlements. This figure shows that this elasticity approach predicts settlements for footings on stiff clay, which compare very well with the measured settlements.

The validity of the chart by Jambu et al. *(21)* has been challenged by Christian and Carrier *(23)*. The use of the modi-

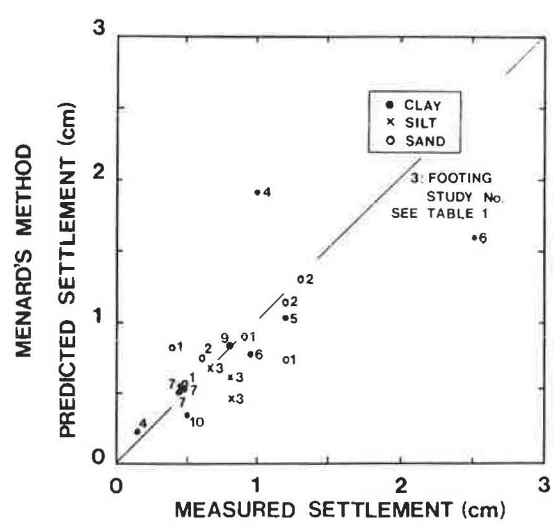

FIGURE 21 Measured versus predicted settlement by Menard's method.

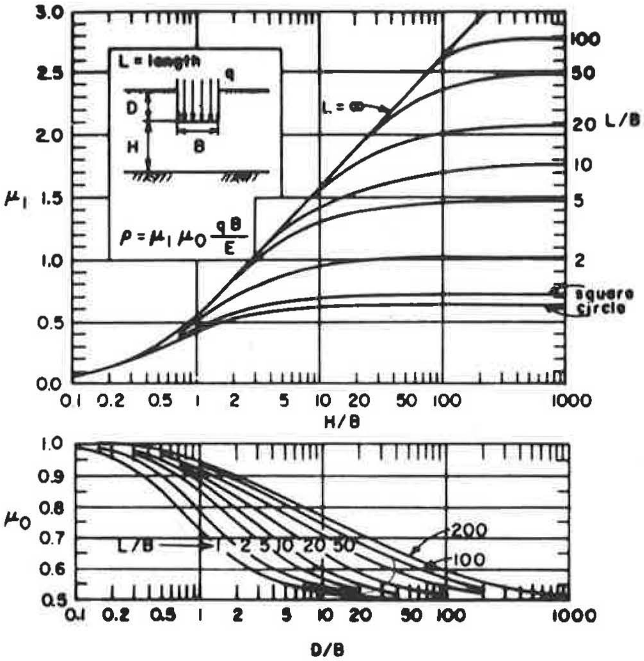

FIGURE 22 Jambu-Bjerrum-Kjaernsli chart *(21).*

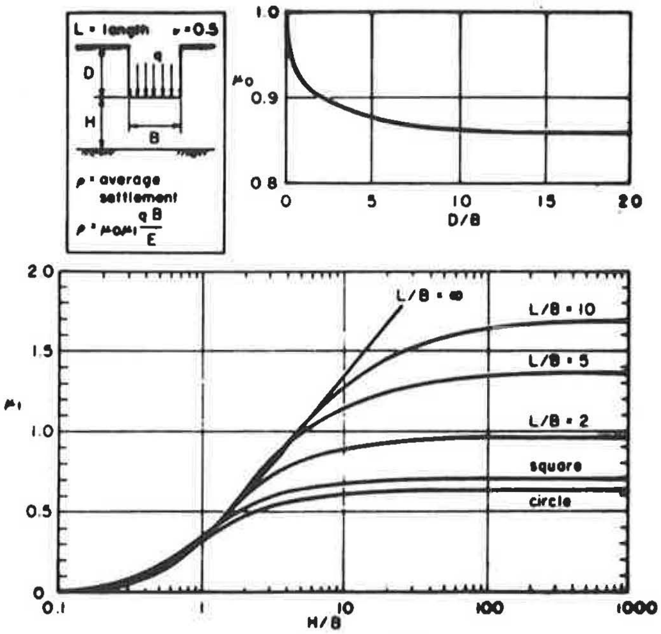

FIGURE 24 Christian carrier chart *(23).*

fied chart proposed by Christian and Carrier (Figure 24) will generally lead to higher predicted settlement; note that this chart applies only to a Poisson's ratio of 0.5.

SETTLEMENT: GENERAL BEHAVIOR

The 17 load test results presented in Figures 5 to 14 can be regrouped on a normalized load settlement plot (Figure 25). The load is normalized to the ultimate load at a settlement of one-tenth of the footing width; the settlement is normalized to one-tenth of the footing width. The resulting curves fall within the band shown in Figure 25 indicating that with a factor of safety of 3, the settlements for the load tests on stiff clay were 0.5 to 1 percent of the footing width.

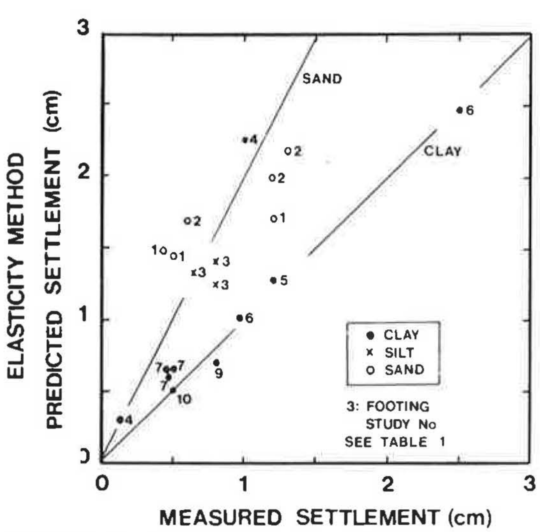

FIGURE 23 Measured versus predicted settlement by elasticity method.

CONCLUSIONS

Load test results on shallow footings varying from 0.30 m to 2.41 m (1 ft to 7.9 ft) have been presented together with predicted behavior using preboring pressuremeter test results.

The ultimate bearing pressure is defined as the pressure reached at a settlement equal to one-tenth of the footing width, the measured values of ultimate bearing pressure allowed to propose new simplified bearing capacity design curves. These curves are somewhat more conservative than the previously existing design curves. The ratio of predicted overmeasured bearing capacity using new pressuremeter rules varies from 0.60 to 1.24 (Figure 15). The same ratio using the general bearing capacity equation varies from 0.51 to 1.67 in clay and from 0.12 to 12 in sand (Figures 16 and 17).

The settlement at one-third of the ultimate bearing pressure predicted by Menard's method compared relatively well with the measured settlement. The precision of the Menard settle-

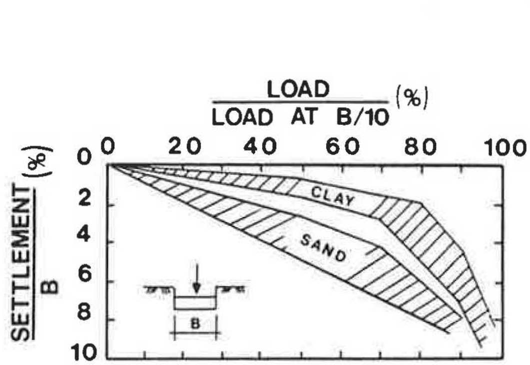

FIGURE 25 General behavior of footings.

ment predictions is about + 50 percent (Figures 20 and 21). An elasticity approach is proposed to predict settlement; this approach is promising (Figure 23), however, more work is required in order to fully evaluate its potential.

REFERENCES

1. J. L. Briaud and M. Gambin. Suggested Practice for Drilling Boreholes for Pressuremeter Testing. *ASTM Geotechnical Testing Journal,* Vol. 7, No. 1, 1984.
2. J. L. Briaud, L. M. Tucker, and R. S. Olsen. Pressuremeter and Foundation Design. Short Course Notes, Vol. 1, Civil Engineering Department, Texas A&M University, College Station, 1982.
3. E. Winter. Suggested Practice for Pressuremeter Testing in Soils. *ASTM Geotechnical Testing Journal,* Vol. 5, No. 3/4, 1982.
4. J. L. Briaud, A. Noubani, J. Kilgore, and L. M. Tucker. Correlations Between Pressuremeter Data and Other Soil Parameters. *Research Report.* Civil Engineering Department, Texas A&M University, College Station, Nov. 1985.
5. L. Menard. Calcul de la Force Portante des Fondations sur la Base des Resultats des Essais Pressiometriques. *Sols-Soils,* Vol. 2, Nos. 5 and 6, 1963.
6. A. W. Skempton. The Bearing Capacity of Clays. *Proc., Building Research Congress,* Vol. 1, 1951.
7. A. S. Vesic. Expansion of Cavities in Infinite Soil Mass. *Journal of the Soil Mechanics and Foundation Engineering Division, ASCE,* Vol. 98, No. SM3, 1972.
8. F. Baguelin, J. F. Jezequel, and D. H. Shields. *The Pressuremeter and Foundation Engineering.* Trans Tech Publications, Rockport, Mass., 1978.
9. D. H. Shields and G. E. Bauer. Determination of the Modulus of Deformation of a Sensitive Clay Using Laboratory and In Situ Tests. *ASCE Specialty Conference on In Situ Measurement of Soil Properties.* North Carolina State University, Raleigh, 1975.
10. M. W. O'Neill and S. A. Sheikh. Geotechnical Behavior of Underreams in Pleistocene Clay. *Proc., Session on Drilled Piers and Caisson II,* ASCE Convention, Denver, Colo., May 1985.
11. J. L. Briaud and K. Riner. A Study of Cyclic Pressuremeter Testing for Offshore Applications. *Research Report 4839.* Civil Engineering, Texas A&M University, College Station, 1984.
12. M. W. O'Neill and L. C. Reese. Behavior of Axially Loaded Drilled Shafts in Beaumont Clay. *Research Report 89-8.* Center for Highway Research, University of Texas, Austin, 1970.
13. Woodward Clyde Consultants. *Study to Investigate the Effects of Skin Friction on the Performance of Drilled Shafts in Cohesive Soils.* U.S. Army Waterways Experiment Station, Vicksburg, Miss., Aug. 1981.
14. K. E. Tand, E. G. Funegard, and J. L. Briaud. Bearing Capacity of Footings on Clay: CPT Method. *Use of In Situ Tests in Geotechnical Engineering,* ASCE Specialty Conference, Blacksburg, Va., 1986.
15. Briaud Engineers. Foundation Investigations Using Pressuremeter Testing at Chocolate Bayou and Texas City Amoco Plants. Kenneth E. Tand and Associates, Inc., Houston, Tex., Jan. 1984.
16. A. Marsland and M. F. Randolph. Comparison of the Results from Pressuremeter Tests and Large In Situ Plate Tests in London Clay. *Geotechnique,* Vol. 27, No. 2, 1977, pp. 217–243.
17. L. D. Johnson. Correlation of Soil Parameters from In Situ and Laboratory Tests for Building 333. *Use of In Situ Tests in Geotechnical Engineering,* ASCE Specialty Conference, Blacksburg, Va., 1986.
18. S. Amar, F. Baguelin, and Y. Canepa. Etude Experimentale du Comportement des Fondations Superficelles. *Annales de l' I.T.B.T.P. 427.* Serie Sols et Fondations 189, Sept. 1984.
19. L. Menard and J. Rousseau. L'Evaluation des Tassements-Tendances Nouvelles. *Sols-Soils,* Vol. 1, No. 1, 1962.
20. L. Menard. The Menard Pressuremeter: Interpretation and Application of Pressuremeter Test Results to Foundation Design. *Sols-Soils,* No. 26, 1975.
21. N. Jambu, L. Bjerrum, and B. Kjaernsli. *Guidance in the Solution of Foundation Problems.* Publication 16. Norwegian Geotechnical Institute, Oslo, 1956.
22. J. H. Schmertmann. Improved Strain Influence Factor Diagram. Technical Note. *Journal of the Soil Mechanics and Foundation Engineering Division, ASCE,* Vol. 104, No. BT8, 1978.
23. J. T. Christian and W. D. Carrier. Jambu, Bjerrum, and Kjaernsli's Chart Reinterpreted. *Canadian Geotechnical Journal,* Vol. 15, 1978, pp. 123–128.
24. J. H. Deschenes. *Bearing Capacity of Footings Close to Slopes of Cohesionless Soil.* Ph.D. dissertation. Civil Engineering, University of Ottawa, Canada, 1978.
25. J. L. Briaud. *The Pressuremeter: Application to Pavement Design.* Ph.D. dissertation. Department of Civil Engineering, University of Ottawa, Canada, 1979.

Publication of this paper sponsored by Committee on Foundations of Bridges and Other Structures.